Macromolecules

ARTICLE

pubs.acs.org/Macromolecules

Effects of Tricresylphosphate on Gas Transport Coefficients in Matrimid and 6FDA-TMPD Polyimides

Carolina García, Mar López-González, Javier de Abajo,* Leoncio Garrido, and Julio Guzmán*

Instituto de Ciencia y Tecnología de Polímeros (CSIC), Juan de la Cierva 3, 28006 Madrid, Spain

ABSTRACT: Membranes were prepared with two polyimides (Matrimid and 6FDA-TMPD) having a content of tricresylphosphate ranging from 0 to 33% (w/w). The specific volumes of these membranes were used to determine the partial specific volume of tricresylphosphate in the membranes, the hypothetical specific volumes of the pure polyimides in the liquid state and the fraction of nonequilibrium excess free volume in the glassy state. Permeation measurements were carried out and the gas transport coefficients for oxygen, carbon dioxide and nitrogen were determined. Sorption experiments of carbon dioxide were also performed in tricresylphosphate and in neat 6FDA-TMPD polyimide membrane. Additionally, the solubility and diffusion coefficients of $[^{13}C]O_2$ in the same materials were determined with ^{13}C pulsed field gradient NMR measurements. The analysis of the gas transport coefficients of the membranes as a function of the content in tricresylphosphate clearly showed an important decrease in solubility and permeability but with little influence on the permselectivity.

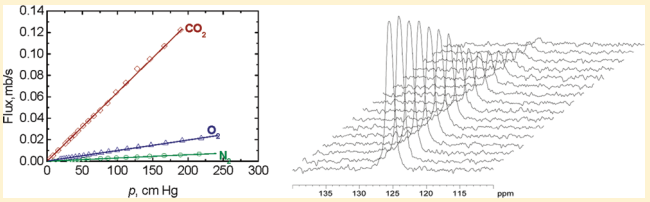

INTRODUCTION

Glassy polymers that exhibit high glass transition temperatures (T_g) have become the preferred materials for the preparation and evaluation of gas separation polymer membranes.[1−3] In this context, polyimides have achieved special significance as they exhibit very high values of T_g along with a very favorable balance of physical properties, such as thermal stability, mechanical resistance and acceptable processability. Polyimides are promising membrane materials thanks to their inherent molecular rigidity, which favors a suitable size-sieving ability, and to their specific interactions with individual gases.[4−8]

Plasticization and antiplasticization are physical phenomena repeatedly observed when studying the permeation characteristics of polymer membranes and, particularly, polyimide membranes. Plasticization can be promoted by condensing gases and vapors, such as CO_2 and light hydrocarbons, and it is an undesired effect that negatively affects the separation capabilities of membranes. Polymers affected by plasticization at high pressures are not useful materials for technical applications. On the other hand, antiplasticization can be beneficial when polymers are used as barrier materials.

The term antiplasticization has been used for at least two forms of modification of polymer membranes. On one hand, antiplasticization could be understood as the effect of diluents or plasticizers on the gas permeability of polymer membranes[9−11] and, on the other, antiplasticization could also been defined as the beneficial effect achieved by means of polymer cross-linking, referring to the plasticization observed for many glassy polymer membranes by CO_2 and by other gases and vapors.[12−18]

The effect of low molecular weight diluents or plasticizers on transport properties has been studied in the past and the mechanisms which govern the changes in physical properties such as free volume, glass transition temperature or gas/polymer affinity have been analyzed to explain the intricacy of the polymer−plasticizer interaction and its effect on the separation phenomena. For instance, it is not readily understood how the intrinsic characteristics of the polymer material are modified, since the loss of permeability caused by antiplasticization does not always result in a gain in selectivity, as it would be expected in order to comply with the trade-off between productivity and selectivity.

To investigate the effect of the plasticizer tricresylphosphate on the permeation characteristics of polyimides, a technical polyimide, Matrimid, and an experimental polyimide, 6FDA-TMPD, were selected. Matrimid is probably the technical polyimide which shows the best behavior as a gas separation polymer membrane, while the polyimide 6FDA-TMPD has been previously reported as one of the most suitable materials for this application in terms of the permeability/selectivity trade-off. Both polyimides are among those which exhibit the highest permeability to CO_2, and although both plasticize at relatively high pressure, antiplasticization by the addition of diluents has not been studied for these polymers.

EXPERIMENTAL PART

Polymer Materials and Dense Membranes. Tricresylphosphate from Bayer (bp = 240−255 °C at 4 mmHg.) and the technical polyimide Matrimid (Huntsman) were used as received. The experimental polyimide was synthesized from hexafluoroisopropylidene

Received: March 15, 2011
Revised: April 4, 2011
Published: April 18, 2011

dx.doi.org/10.1021/ma2005876 | *Macromolecules* 2011, 44, 3862–3873

Scheme 1. Repeating Unit of Polyimides Chemical Structures

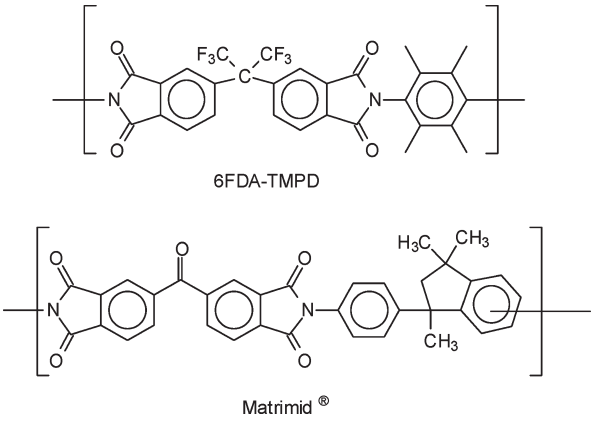

diphthalic anhydride (6FDA) and 2,3,5,6-tetramethyl-1,4-diaminobenzene (durenediamine, TMPD) by the general two-step polyimidation procedure. The chemical structures of both polyimides are given in Scheme 1.

An improved synthetic route was applied, which involved the use of pyridine and trimethylchlorosilane as reaction rate promoters.[19] Using this method, quantitative yields and high molecular weights were achieved. The inherent viscosities of the polyimides were determined at 25 °C with an Ubbelhode viscometer in *N*-methyl-2-pyrrolidinone (NMP) solutions at a concentration of 0.5 g/dL. Gel permeation chromatography analyses were carried out with a device equipped with Resipore (250 × 4.6 mm, 3 μm nominal particle size) Polymer Laboratories columns. DMF containing 0.1% LiBr was used as solvent. Measurements were performed at 70 °C at a flow rate of 0.3 mL/min using an IR detector. The molecular weights of the polymers were referenced to poly(ethylene glycol) standars: Matrimid (η = 0.52 dL/g); 6FDA-TMPD (η = 0.93 dL/g, M_n = 72300 and M_w/M_n = 2.8).

Membranes were prepared by casting filtered solutions of varying polymer/plasticizer ratio. The solutions were cast on balanced glass plates which were fixed to a heating plate. Chloroform was used as the solvent for Matrimid and *N*-methyl-2-pyrrolidinone (NMP) was used for 6FDA-TMPD. Most solvent was removed slowly over 24 h, at room temperature and 80 °C for chloroform and NMP, respectively. Polymer films were then stripped off and the rest of the solvent was removed in a vacuum oven following the same heating protocol for both membranes: 180 °C/24 h and 24 h at 250 °C. As a result, a negligible amount of solvent remained, as confirmed by thermogravimetric analysis (TGA).

For this study, a set of dense membranes were prepared with thicknesses ranging from 40 to 50 μm. Increasing amounts of the diluent tricresylphosphate (TCP) were added to the polymer, from 5% to a maximum of 50% (w/w).

Characterization of the Membranes. *Density Measurements.* The densities of the films were determined by the flotation method at 20 °C using water and an aqueous solution saturated with $ZnCl_2$. The composition of the solution was adjusted to maintain the films suspended throughout. Care was taken to eliminate all bubbles adhering to the films using an ultrasonic bath. To minimize the error, four different pieces for each polymer were employed. The densities of the solutions were determined using a pycnometer, and the experimental error was estimated to be less than 0.002 g/cm^3.

Glass Transition Temperatures. The glass transition temperatures were determined by calorimetric measurements performed in a TA Instruments TA-Q-2000 differential scanning calorimeter. Samples of about 10 mg were heated up to 450 °C under nitrogen atmosphere at 20 °C/min and quenched with a cooling rate of 200 °C/min. The T_g values reported were estimated from the second heating cycles (heating rate = 15 °C/min) and correspond to the midpoint of the thermal step in the DSC curves.

Permeation Measurements. A laboratory-made permeator, described elsewhere,[20] was used for permeation measurements. Briefly, it consists of a gas cell in which the polymer membrane is placed in the center, separating the high-pressure or upstream chamber from the low-pressure or downstream chamber. High vacuum was generated in the permeation device by means of an Edwards molecular turbo-pump and the whole arrangement was thermostatically controlled at 30 °C by means of a water bath. Before performing the measurements, vacuum was maintained overnight in the permeation device to remove the last traces of solvent and gas in the membrane, and to reach a low pressure (about 10^{-6} bar). Subsequently, gas contained in a reservoir was allowed to flow into the downstream chamber and the evolution of the pressure of the gas in this chamber was monitored with a MKS Baratron type 627B absolute pressure transducer working in the pressure range 10^{-4}−1 mmHg. Pressure in the upstream chamber was measured with a Gometrics transducer to control the gas pressures at which the experiments are performed, which varied between 0.1 and 5 bar in this work. Three independent experiments were performed for each membrane and gas.

The permeability and diffusivity coefficients were calculated from the curves measuring the pressure increase at the downstream side, recorded at intervals of 1 s. For each experiment, the intake of air into the evacuated downstream chamber was measured as a function of time and subtracted from the curves representing the pressure of permeant against time in the downstream chamber.

The gases employed in the transport measurements, all with purity higher than 99%, were nitrogen, oxygen, and carbon dioxide.

Sorption Measurements. Sorption measurements were carried out at 30 °C to determine the concentration of gas in the polyimide membranes, as well as in the liquid TCP at different pressures. An experimental device consisting of a gas reservoir separated from the sorption chamber by a valve was used.[21] The reservoir and the sorption chamber equipped, respectively, with Gometrics (0−35 bar) and MKS-722 (0−33 atm) pressure sensors were immersed in a thermostat at the temperature of interest. At the beginning, the sample was placed inside the sorption chamber and exposed to vacuum overnight, at 30 °C, to remove air. Then gas, at a given pressure, was introduced into the reservoir and, once it reached the temperature of interest, the valve separating the reservoir and the sorption chamber was suddenly opened and closed. The decrease of the gas pressure in the sorption chamber was recorded every second with a PC via a precision pressure indicator. After reaching a constant pressure, an additional amount of gas was introduced into the sorption chamber and, then, allowed to reach equilibrium again, and so forth. Thus, gas sorption was measured as a function of pressure using compressibility factors to determine the concentration of gas in the liquid. The sorption measurements at 30 °C and several pressures were performed. Pressure leaks and the adsorption of gas in the chamber walls were measured previously in blank experiments.

Diffusion Measurements by ^{13}C PFG-NMR in Tricresyl Phosphate and in 6FDA-TMPD Membranes. *PFG NMR Experiments.* An amount (~1.5 g) of the liquid plasticizer tricresyl phosphate or membrane strips less than 2 mm wide and approximately 2 cm long were placed inside a 10 mm o.d. NMR tube designed for NMR studies of moderately pressurized gases. In addition, a standard consisting of a sealed glass capillary with a known amount of [^{13}C(1)] labeled (99%, Euriso-top, Gif-sur-Yvette, France) acetic acid was placed in the tube. Prior to fill the tube at a given pressure with [^{13}C]O_2 (99%, Cambridge Isotopes Laboratories, Andover, MA), the air was removed by vacuum. Unless indicated, the gas pressure used in these experiments was in the range of 2 to 4 bar to facilitate the measurements with adequate signal-to-noise ratio in a reasonable amount of time. The gas pressure was

Table 1. Weight Fraction of Tricresylphosphate, Specific Volumes, and Glass Transition Temperatures of the Matrimid Membranes

Matrimid	TCP $(1 - w_p)$ feed	TCP $(1 - w_p)$ by TGA	V_{sp} (cm^3/g)	T^*_g (K)[a]	T_g (K) DSC
1	0	0	0.8025	578	578
2	0.05	0.04	0.7952	541	523
3	0.16	0.155	0.7852	456	463
4	0.20	0.197	0.7880	431	447
5	0.33	0.358	0.7839	357	402
6	0.50	0.336	0.7759	366	382
7	1	1	0.8584	212	

[a] T^*_g: calculated values of the glass transition temperatures according to the Fox equation.

Table 2. Weight Fraction of Tricresylphosphate, Specific Volumes, and Glass Transition Temperatures of the 6FDA-TMPD Membranes

6FDA-TMPD	TCP $(1 - w_p)$ feed	TCP $(1 - w_p)$ by TGA	V_{sp} (cm^3/g)	T^*_g (K)[a]	T_g (K) DSC
1	0	0	0.7701	693	693
2	0.05	0.05	0.7726	622	640
3	0.16	0.157	0.7530	511	570
4	0.20	0.177	0.7442	494	546
5	0.33	0.264	0.7458	433	514
6	0.50	0.22	0.7766	462	527
7	1	1	0.8584	212	

[a] T^*_g: calculated values of the glass transition temperatures according to the Fox equation.

monitored with a transducer working in the range 0−10 bar. The diffusion coefficient of the gas in the membranes was estimated by a spin echo type of radiofrequency (rf) pulse sequence, as shown by Stejskal et al.[22] The measurements were performed in a Bruker Avance 400 spectrometer equipped with a 89 mm wide bore, 9.4 T superconducting magnet (^{13}C Larmor frequency at 100.61 MHz). The reported data were acquired at 30 ± 1 °C with a Bruker diffusion probehead Diff60 using 90° ^{13}C rf pulse lengths of about 13 μs. An inversion−recovery pulse sequence was used to estimate the ^{13}C longitudinal relaxation times, T_1, of sorbed gas. Solubility measurements were performed by acquiring ^{13}C NMR spectra of samples using a single pulse excitation sequence with a repetition rate $\geq 5 \times T_1$. For diffusion measurements, a pulsed field gradient stimulated spin echo pulse sequence was used. The echo time between the first two 90° rf pulses, τ_1, varied between 2.11 and 3.11 ms. The apparent diffusion coefficient of $[^{13}C]O_2$, D, was measured at diffusion times, Δ, of 20, 240, or 500 ms. The length of the field gradient pulses, δ, was 1 or 2 ms. For a set of δ and Δ values, the amplitude of the gradient pulses varied from 0 up to a maximum value of 20 T m^{-1}. The repetition rate was $\geq 5 \times T_1$. The total acquisition time for these experiments ranged from 3.5 to 87 h. Self-diffusion coefficients were calculated by fitting the experimental data to the corresponding exponential function. All ^{13}C NMR spectra were referenced to $^{13}C(1)$ acetic acid (178.1 ppm), secondary to tetramethylsilane (0.0 ppm).

Previous to these measurements, the field gradient was calibrated following the spectrometer manufacturer's protocol at 25 ± 1 °C, using a sample of water doped with $CuSO_4$ at 1.0 g l^{-1} and a value of the water diffusion coefficient equal to 2.3×10^{-5} cm^2 s^{-1}. Furthermore, the calibration was verified at the range of gradient values used experimentally by measuring the diffusion coefficient of dry glycerol. It was found a value of $D = 2.23 \times 10^{-8}$ cm^2 s^{-1}, in good agreement with the results reported for this parameter elsewhere.[23] Also, diffusion measurements for these two liquids were performed over a wide range of diffusion times to assess the stability of the gradients and whether artifacts due to eddy currents could affect the measurements. The temperature at the sample volume in the probe head was determined by measuring the difference between the proton chemical shifts of a solution of ethylene glycol at 80% v/v in deuterated dimethyl sulfoxide.

With the experimental system indicated above and using the internal standard concentration, it was possible to determine both the solubility and diffusion coefficients of the gas in TCP and in the polyimide membranes and, consequently, from the product between the solubility and diffusion coefficients, the corresponding permeability coefficients. Thus, all the gas transport coefficients can be determined from NMR measurements.

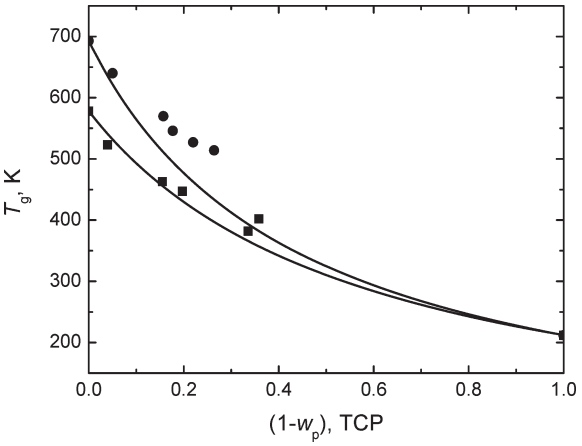

Figure 1. Experimental (symbols) and calculated (continuous lines) glass transition temperatures for the Matrimid (squares) and 6FDA-TMPD (circles) blends with tricresylphosphate (TCP).

RESULTS AND DISCUSSION

Characteristics and Properties of the Membranes. Tables 1 and 2 summarize the main characteristics of the membranes used in this work. The second and third columns show the values of the weight fraction of TCP in the feed, and that determined from thermogravimetric analysis after the casting of the membranes, respectively. A relatively good agreement between both values was observed, except for the membranes with the highest weight fractions of TCP which exhibited extremely high differences, suggesting that the maximum weight fraction of TCP that can be added to the polyimides is about 0.33 for Matrimid and 0.25 for the 6FDA/TMPD.

The glass transition temperatures of the blends of polyimides with tricresylphosphate as a function of the weight fraction of TCP are shown in Figure 1, as well as the curves calculated according to the Fox equation for the glass transition temperatures of homogeneous blends. For the calculations, the T_g of TCP was taken as 212 K.[24] Apparently two different behaviors can be observed: for Matrimid/TCP blends, the Fox equation is valid, whereas for the 6FDA-TMPD/TCP blends, important deviations were observed, even at temperatures above 80 K.

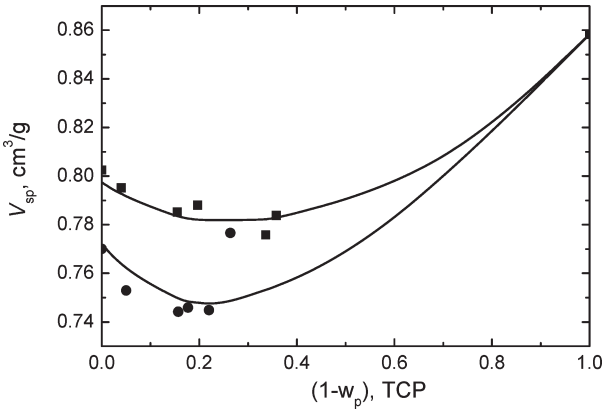

Figure 2. Variation of the specific volume with the weight fraction of tricresylphosphate $(1 - w_p)$ for the Matrimid (squares) and 6FDA-TMPD (circles) membranes. The lines correspond to predicted values according to the model proposed by Ruiz-Treviño and Paul.[25]

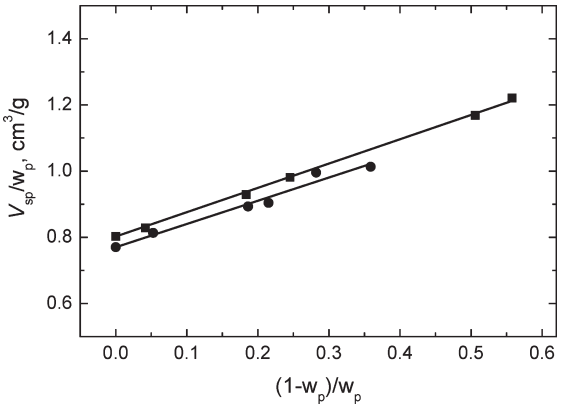

Figure 3. Graphical procedure for the determination of the TCP partial specific volume by using the data of Tables 1 and 2 in the Matrimid and 6FDA membranes. The symbols retain the same meaning as in Figure 2.

However, since the T_g of 6FDA-TMPD/TCP blends are very high, it is possible that migration of the plasticizer takes place due to the high vapor pressure of TCP at these elevated temperatures, hampering an adequate determination of the true value of T_g by the calorimetric method. Therefore, in our opinion it is more reasonable to consider the values of T_g calculated by the Fox equation.

Specific Volumes of the Membranes in the Glass and Liquid States. Values of the specific volume of the membranes are illustrated as a function of the weight fraction of TCP in Figure 2.

It can be observed that the specific volume of the plasticized membranes (V_{spg}) in the glassy state is lower than that of the polyimide itself up to weight fractions of TCP lower than 0.3, indicating a negative excess specific volume.

The model developed by Ruiz-Treviño and Paul[25] was used to calculate the best fits to the experimental results (Figure 2). Knowing the glass transition temperatures of the plasticized and pure polymers, and their corresponding weight fractions, and assuming that the differences of thermal expansion coefficients ($\Delta\alpha$) between the liquid and the glass state is a constant for each series of polymer and plasticized membranes, values of the hypothetical specific volume in the liquid state (V^0_{spl}) for Matrimid and 6FDA-TMPD of 0.71 and 0.65 cm^3/g, respectively, were estimated, whereas a value of $\Delta\alpha$ of approximately 3×10^{-4} cm^3/g K was appropriate for all membranes. With these values, the fraction of nonequilibrium excess free volume in the glassy state can be determined from:

$$f_g = \frac{V^0_{spg} - V^0_{spl}}{V^0_{spg}} = \frac{\Delta V_{excess}}{V^0_{spg}} \qquad (1)$$

For Matrimid and 6FDA-TMPD, the values of f_g were 0.13 and 0.184, respectively. In terms of gas adsorption, these represent the maximum volume fraction accessible to gas penetration as Langmuir sites. The difference between both values is due to the lower glass transition temperature of the former polymer. At the same time, f_g can also be determined by the equation

$$f_g = \frac{\Delta V_{excess}}{V^0_{spg}} = \frac{\Delta\alpha(T_g - T)}{V^0_{spg}} \qquad (2)$$

obtaining values of 0.103 and 0.164 for Matrimid and 6FDA-TMPD, respectively, slightly lower than those indicated above.

Partial Specific Volume of TCP in the Membranes. As outlined by Maeda and Paul,[26] the partial specific volume of TCP in the mixture ($\overline{V}_{TCP}$) can be obtained from the slopes of the plots of volume of the mixture per unit mass of polymer, V_{sp}/w_p, vs. the mass of TCP in the mixture per unit mass of polymer $(1 - w_p)/w_p$ (Figure 3).

The values obtained were 0.735 and 0.702 cm^3/g for Matrimid and 6FDA-TMPD, respectively, and were much lower than in pure liquids, such as toluene, methylethylketone and trichloroethylene, where $\overline{V}_{TCP}$ is practically identical to that of the pure tricresylphosphate. The values of $\overline{V}_{TCP}$ are also lower than those found by Maeda and Paul for tricresylphosphate in polysulfone,[26] although similar conclusions with respect to the role of the plasticizer in the polymer blend could be derived from both studies. The results of partial specific volumes (higher than zero) contradict the argument that the diluent molecules fill the interstitial spaces between polymer chains without increasing volume and, consequently, do not serve to interpret sorption and transport behavior in plasticized systems.

Permeability, Diffusion, and Solubility Coefficients. The solubility coefficients of CO_2 in liquid TCP and of CO_2 and O_2 in the pure 6FDA-TMPD membrane were determined from sorption measurements by using the experimental device indicated above. The concentration of gas, in cm^3(STP)/cm^3 of sample, is given by

$$C = \frac{22414\rho V}{RTm}\left(\frac{p_i}{z_i} - \frac{p_e}{z_e}\right) \qquad (3)$$

where m and ρ are, respectively, the mass and density of the sample, V is the unoccupied volume of the sorption chamber, R and T are the gas constant and absolute temperature and p and z are, respectively, the pressure and compressibility coefficient of the gas. The subscripts, i and e refer, respectively, to the initial and equilibrium conditions.

The pressure dependence of the concentration of gas in TCP and in the 6FDA-TMPD membrane is shown in Figure 4.

The curves exhibit the usual pattern displayed by the sorption of gases in this kind of materials, that is, the isotherms are convex with respect to the abscissa axis in the case of the liquid TCP, whereas in the case of the glassy polyimide membrane, the contrary occurs with concave isotherms with respect to the

pressure axis. Table 3 shows data of the solubility coefficients extracted from the first derivative of the variation of C with pressure at infinite dilution (zero pressure). Obviously, the solubility coefficients at different pressures can also be determined from the experimental curves.

NMR measurements were also used to determine the transport coefficients in the polyimide membranes, as well as in the plasticizer TCP. In the polyimide membranes, the ^{13}C NMR spectra of samples with the standard showed three peaks, as illustrated in Figure 5.

One peak corresponding to the ^{13}C signal of the carboxyl group of acetic acid at 178.1 ppm, and two peaks associated with the $[^{13}C]O_2$ in the membranes, centered at 128.6 and 125.6 ppm. These two peaks reflect the existence of two populations of $[^{13}C]O_2$ corresponding, respectively, to the nonsorbed (free) and sorbed (in the membrane) gas fractions, in a slow exchange regime. In the case of TCP, only one peak of $[^{13}C]O_2$ was observed associated with the sorbed gas in the liquid, since the active volume defined by the radiofrequency coil in the probe is occupied mainly by the TCP. The peak at lower frequency (sorbed gas) arises from interaction between the polymer or TCP and gas molecules which have a highly polarizable C═O bond. The estimated spin−lattice relaxation times, T_1, of sorbed gas in the membranes was ~2.6 s. The free gas exhibits T_1 values in the range of 50 to 65 ms. Thus, in all NMR measurements, repetition rates $\geq 5 \times T_1$ of sorbed gas were used. After reaching equilibrium conditions, the solubility of $[^{13}C]O_2$ in the 6FDA-TMPD membrane and in TCP was determined by comparing the areas of the peaks associated with the reference compound ($^{13}C(1)$ labeled acetic acid) and the sorbed gas in the corresponding ^{13}C NMR spectra. The results are summarized in Table 3.

A PFG stimulated spin echo sequence was used to determine the diffusion coefficient of CO_2 in the membranes. The choice of this type of pulse sequence and the set of time parameters used in the diffusion experiments were conditioned by the NMR relaxation times of sorbed $[^{13}C]O_2$ in the membranes. Thus, based on our experience[27,28] a compromise was sough in order to achieve a reasonable signal-to-noise ratio with short echo times (2−3 ms) and adequate diffusion times to, at least, attenuate 40% the amplitude of the initial signal. Diffusion times larger than 10 ms properly average the diffusive paths associated with different environments in glassy membranes.[27,28]

The pulse sequence consists of three $\pi/2$ rf pulses timely spaced that generate an observable NMR signal (echo) centered

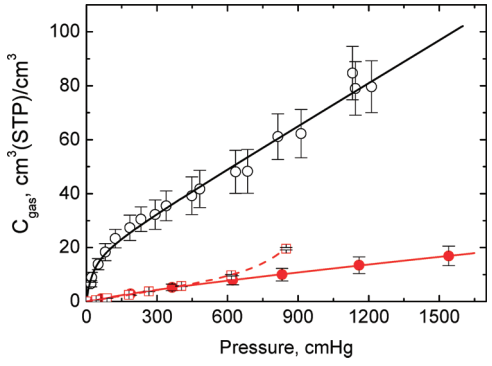

Figure 4. Sorption of carbon dioxide (open circles) and oxygen (filled circles) in 6FDA-TMPD membranes and of carbon dioxide in tricresylphosphate (squares) at 30 °C.

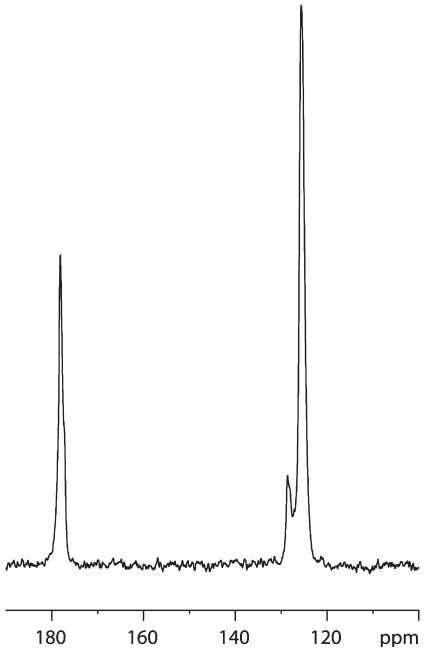

Figure 5. ^{13}C NMR spectra corresponding to a sample of 6FDA-TMPD in the presence of $[^{13}C]O_2$. The peaks at 128.6 and 125.6 ppm correspond to free and sorbed $[^{13}C]O_2$, respectively. The peak at 178.1 ppm is associated with the standard CH_3-$[^{13}C]OOH$.

Table 3. Summary of Sorption and NMR Results at 30 °C

sample	gas and procedure	p bar	S, cm^3 (STP) cm^{-3}cmHg^{-1}	D, cm^2 s^{-1}	P, barrer
TCP	$^{13}CO_2$, NMR	2.38	0.0156	3.6E-6	562
TCP	CO_2, sorption	0−5	0.0142	2.2E-6	312
6FDA-TMPD	$^{13}CO_2$, NMR	0	0.57[a]	1.57E-7[a]	896
6FDA-TMPD	$^{13}CO_2$, NMR	1.13	0.375	2.23E-7	837
6FDA-TMPD	$^{13}CO_2$, NMR	2.26	0.326	3.12E-7	1017
6FDA-TMPD	$^{13}CO_2$, NMR	3.40	0.245	3.39E-7	831
6FDA-TMPD	CO_2, sorption	0	0.706[a]		
6FDA-TMPD	CO_2, sorption	0.67	0.7	2.0E-7	1400
6FDA-TMPD	O_2, sorption	0	0.018[a]		
Matrimid	$^{13}CO_2$, NMR	3.45	0.089	8.4E-9	7

[a] Determined from the variation of S and D with pressure in the limit of zero pressure.

dx.doi.org/10.1021/ma2005876 |*Macromolecules* 2011, 44, 3862–3873

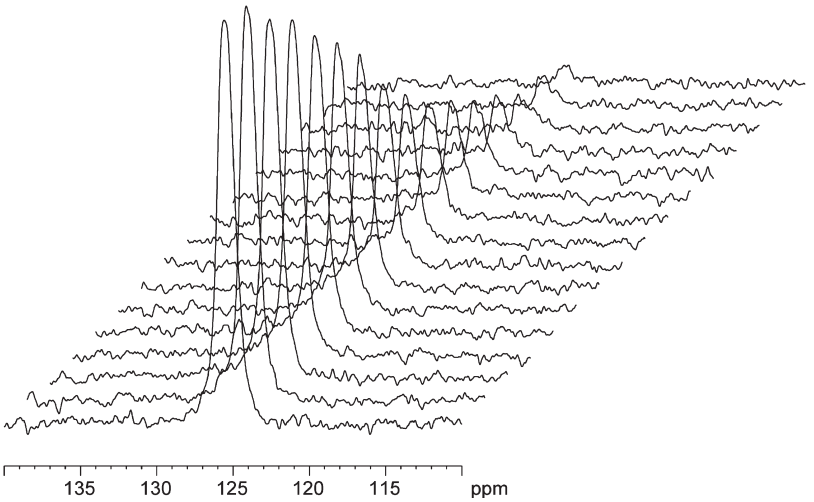

Figure 6. ^{13}C PFG NMR spectra corresponding to $[^{13}C]O_2$ sorbed in 6FDA-TMPD obtained at 30 °C and a gas pressure of 2.26 bar. The duration, δ, of the gradient pulse was 1 ms and the diffusion time, Δ, was 240 ms. The gradient amplitude, g, was incremented in 16 consecutive steps of 60 g cm^{-1} from an initial value of 60 g cm^{-1}.

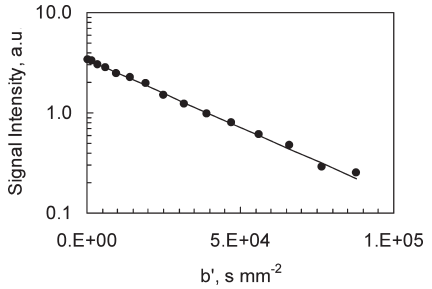

Figure 7. Plot of the peak intensity vs. b' corresponding to $[^{13C}]O_2$ sorbed in 6FDA-TMPD obtained with a diffusion time, Δ, equal to 240 ms. The duration, δ, of the gradient pulse was 1 ms and the amplitude of the gradient, g, in G cm^{-1}, varied between 60 and 960. The temperature was 30 °C with a gas pressure of 2.26 bar. The solid line represents the fit to eq 4.

at a time equal to $2\tau_1 + \tau_2$ (stimulated spin echo) from the first rf pulse, where τ_1 is the time separation between the first two rf pulses and τ_2 is the time elapsed between the second and the third rf pulses. The magnetic labeling is accomplished by applying two field gradient pulses of amplitude and duration g and δ, respectively, spaced by a time Δ, the diffusion time. In the absence of motion, the loss of phase coherence of the NMR signal caused by the first gradient pulse would be compensated by the second gradient pulse, but this would not be the case if molecular diffusion occurs during the time Δ. For illustrative purposes, ^{13}C PFG NMR spectra corresponding to $[^{13}C]O_2$ sorbed in 6F-durene are shown as a function the amplitude of the field gradient in Figure 6.

The echo attenuation can be written as follows:[22]

$$A(g) = A(0)\exp[-(b'D)] \quad (4)$$

where $A(g)$ and $A(0)$ are the amplitude of the echo in the presence of a gradient pulse with amplitude g and 0, respectively, $b' = (\gamma g\delta)^2(\Delta - \delta/3)$ where γ is the gyromagnetic ratio of the nucleus being observed, Δ and D are, respectively, the diffusion time and the self-diffusion coefficient of the sorbed gas, and δ is the duration of the gradient pulse. Figure 7 illustrates the attenuation of the echo intensity with increasing values of b',

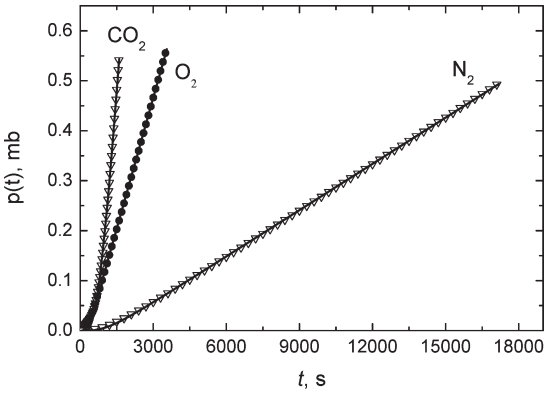

Figure 8. Gas pressure increase measured for carbon dioxide, oxygen and nitrogen in the downstream chamber for Matrimid at $p = 1$ bar in the upstream chamber. The solid lines correspond to the best fits obtained by using eq 5 (solid lines).

keeping Δ and δ constant. In Table 3, the results at various pressures are shown. The diffusional behavior of $[^{13}C]O_2$ in this fluorinated polyimide is similar to that observed in polyethylene above its glass transition temperature, T_g.[27]

The pressure procedure indicated in the Experimental Part has also been used to determine the transport and solubility coefficients of the membranes. Illustrative plots showing the variation of the pressure with time for different gases in the downstream chamber are presented, as an example, in Figure 8 for the Matrimid membrane.

The time dependence of the pressure of the gas in the downstream chamber is deduced by the integration of Fick's second law, and by using appropriate boundary conditions one obtains[29]

$$p(t) = 0.2786\frac{pALST}{V}\left(\frac{Dt}{L^2} - \frac{1}{6} - \frac{2}{\pi^2}\sum_{n=1}^{\infty}\frac{-1}{n^2}\exp\left(-\frac{Dn^2\pi^2 t}{L^2}\right)\right) \quad (5)$$

In this equation, $p(t)$ and p, which denote the pressures of gas in the downstream and upstream chambers respectively, are

dx.doi.org/10.1021/ma2005876 |Macromolecules 2011, 44, 3862–3873

given in cm Hg, A and L represent the area and thickness of the membrane in cm^2 and cm, respectively, the volume of the downstream chamber, V, in cm^3, and D and S are the diffusion and solubility coefficients in cm^2/s and cm^3 gas (STP)/(cm^3 polymer cmHg), respectively. Once steady-state conditions are reached, the time dependence of the pressure of the downstream chamber can be written as

$$p(t) = 0.2786\frac{pALST}{V}\left(\frac{Dt}{L^2} - \frac{1}{6}\right) \quad (6)$$

Plots of $p(t)$ against t in the steady state are straight lines intercepting the abscissa axis at

$$D = \frac{L^2}{6\theta} \quad (7)$$

where θ is the time lag, and therefore, the diffusion coefficient can be obtained from the eq 7. Assuming that the permeability coefficient, P, is the product of the solubility coefficient and the diffusion coefficient, the value of P in barrers {1 barrer [$10^{-10}$$cm^3$(STP) cm/($cm^2$scmHg)]} can be obtained from eq 8,

$$P = 3.59\frac{VL}{pAT}\lim_{t\to\infty}\left(\frac{dp(t)}{dt}\right) \quad (8)$$

where V, L, and A are given in units of the cgs system and p and $p(t)$ in cmHg.

If the diffusion and permeation coefficients are calculated from the linear pressure increase, characteristic of gas diffusion at the steady state, then the experiment must last long enough to ensure that this steady state is achieved. When the diffusion coefficients are very small, the duration of the experiment is too long for realistic experimental procedures. Thus, for small diffusion coefficients, it is convenient to try the fit of the whole pressure increase curve and to use eq 5 to determine the values of the transport coefficients by using nonlinear regression analysis. In the present work, both procedures were used, essentially to verify that the rise in pressure at the downstream chamber corresponds to Fickian diffusion across the membrane. Equation 5 (including six terms of the summation, although in fact, only four terms of this equation are enough to correctly fit our flow curves) was used to fit the data from experiments carried out with all gases. The transport coefficients obtained from these fits were compared with those calculated from the steady-state straight line, to test that the two sets of coefficients were, within experimental error, comparable. This was indeed the case and Figure 8 shows an example where the experimental pressure curves corresponding to three diffusion experiments performed on Matrimid, and the complete fit of the experimental data points with eq 5 are depicted. The agreement between the transport coefficients obtained from both methods was very good with differences for the diffusion coefficients not exceeding 5% and almost identical permeability values indicating, within the experimental error, the high reliability of both methods.

On the other hand, as can be seen in Figure 9, the values of the stationary flux in the downstream chamber, $\lim_{t\to\infty}((dp(t))/(dt))$, for the different experiments, plotted as a function of the pressure in the upstream chamber, follows straight lines for all the different gases studied, indicating the practical independence of the permeability coefficients in the range of pressures analyzed.

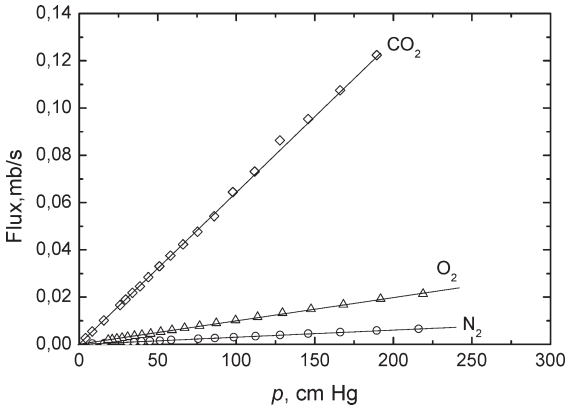

Figure 9. Variation of the stationary flux in the downstream chamber with the gas pressure in the upstream chamber for carbon dioxide, oxygen and nitrogen, for the pure 6FDA-TMPD membrane.

For each experiment, the uncertainties in the diffusion coefficients can be calculated in the following way

$$\sigma = \frac{\left[\left|\frac{L\varepsilon(L)}{3\theta}\right| + \left|\frac{L^2\varepsilon(\theta)}{6\theta^2}\right|\right]}{D} = 2\varepsilon_r(L) + \varepsilon_r(\theta) \quad (9)$$

where $\varepsilon(L)$, $\varepsilon(\theta)$, and $\varepsilon_r(L)$, $\varepsilon_r(\theta)$ are the absolute and relative errors of the corresponding magnitudes.

However, as we have undertaken three experimental runs for each gas and membrane, we prefer to consider the error as the standard deviation of the average values that were about 10% for the diffusion coefficients and 5% for the permeability coefficients.

Once permeability and diffusion coefficients are determined, the solubility coefficients can be calculated directly from the P/D ratio.

With respect to the solubility coefficients in glassy polymers, the solubility of the gas (especially of the most condensing gases) is described by the well-known dual-mode model, which expresses the pressure dependence of the solubility coefficient[30,31]

$$C = k_D p + \frac{[C'_H bp]}{1 + bp} \quad (10)$$

where C is the total concentration of gas in the membrane at pressure p, k_D is the solubility coefficient of the gas in the continuous phase of the glassy material (Henry coefficient), C'_H is the concentration of gas immobilized in Langmuir sites, and b is an affinity parameter accounting for the sorption/desorption ratio.

The values of the different parameters are usually determined by a non linear regression analysis of the experimental curves from eq 10. However, since three unknown parameters intervene in eq 10, it is most convenient to determine k_D previously by other means. In glassy polymers with relatively low glass transition temperatures, the procedure will be to obtain k_D at higher temperatures than T_g and extrapolate to the measurement temperature. Nevertheless, our membranes present high values of T_g, in some cases between 300 and 400 °C, which precludes the use of this method. On the basis of the Flory−Huggins theory for solutions and, following the work of Budzien et al.[32] and Lin and Freeman,[33] the value of k_D, (in cm^3(STP)/cm^3 cm Hg) can be deduced and expressed according to the following

Table 4. Values of Solubility Parameters, Interaction Parameters, Henry Solubility Coefficients, and Langmuir Coefficients for the Carbon Dioxide Sorption in Matrimid Membranes Plasticized with Tricresylphosphate, at 30 °C

Matrimid	TCP $(1 - w_p)$ feed	TCP $(1 - w_p)$ by TGA	χ	δ_2, MPa$^{1/2}$	$10^3 k_D$, cm^3 (STP)/cm^3 cmHg	$C'_H b$, cm^3 (STP)/cm^3 cmHg
1	0	0	1.84	22.1	5.28	0.232
2	0.05	0.04			5.77	0.152
3	0.16	0.155			7.17	0.081
4	0.20	0.197			7.67	0.038
5	0.33	0.358			9.59	0.0105
6	0.50	0.336			9.32	0.0051
7	1	1	0.83	18.8	16,8	0

Table 5. Values of Solubility Parameters, Interaction Parameters, Henry Solubility Coefficients, and Langmuir Coefficients for the Carbon Dioxide Sorption in 6FDA-TMPD Membranes Plasticized with Tricresylphosphate, at 30 °C

6FDA-TMPD	TCP $(1 - w_p)$ feed	TCP $(1 - w_p)$ by TGA	χ	δ_2, MPa$^{1/2}$	$10^3 k_D$, cm^3 (STP)/cm^3 cmHg	$C'_H b$, cm^3 (STP)/cm^3 cmHg
1	0	0	3.78	26.5	0.76	0.545
2	0.05	0.05			1.64	0.461
3	0.16	0.157			3.52	0.232
4	0.20	0.177			3.87	0.170
5	0.33	0.264			5.34	0.089
6	1	1	0.83	18.8	16.8	0

equation:

$$k_D = \frac{22414}{76 p_s V_1} \exp\left[-\left(\left(1 - \frac{1}{N}\right)\phi_2 + \chi \phi_2^2\right)\right] \quad (11)$$

where V_1 is the molar volume of the gas in the liquid state, χ the polymer−solvent interaction parameter, p_s (in atm) is the saturation vapor pressure at the experimental temperature, N is the ratio of the molar volume of the polymer (or plasticizer), to that of the solute (in the pure liquid state), V_2/V_1, and ϕ_2 is the volume fraction of the polymer (or plasticizer).

The values of the interaction parameter χ can be obtained from the solubility parameters by the following equation[34]

$$\chi = \frac{V_1}{RT}(\delta_1 - \delta_2)^2 \quad (12)$$

where V_1 is the molar volume of the solute (the gas in our case) and δ_1 and δ_2 the corresponding solubility parameters of the gas and of the polymer (or plasticizer). Other authors[32] point out that both the regular solution and Flory−Huggins theories suggest that χ is given by

$$\chi = \frac{V_1}{RT}[(\delta_1 - \delta_2)^2 + 2 I_{12} \delta_1 \delta_2] \quad (13)$$

where I_{12} is an additional non-Bertholet mixing parameter that must be taken into account for each gas−polymer pair. However, in this work, as a first approximation, we have considered $I_{12} = 0$ due to the uncertainties involved in the determination of the solubility parameters of the polyimide polymers. For the calculations of χ, V_1 was taken as the partial molar volume for CO_2, $\overline{V}_1 = 46$ cm^3/mol,[35,36] the solubility parameter for CO_2 (12.04 MPa$^{1/2}$ at 303 K) was taken from the work of Camper et al.[37] ($\delta_{CO_2} = -0.0535T$ (K) + 28.26), and the corresponding values for Matrimid (22.1 MPa$^{1/2}$), 6FDA-TMPD (26.5 MPa$^{1/2}$), and Tricresylphosphate (18.82 MPa$^{1/2}$) were taken from Jiang et al.,[38] Kanehashi et al.,[39] and the CRC *Handbook of Lubrication*,[40] respectively.

With these values, we have determined the interaction parameters χ for CO_2 in Matrimid, 6FDA-TMPD polyimide and tricresylphosphate (from eq 12) as well as the corresponding Henry solubility coefficients (from eq 11) by using a value of p_s = 71 atm, determined according to the Antoine equation,[41] or directly from the phase diagram.

The values calculated for χ and k_D are shown in the fourth and sixth columns of Tables 4 and 5. The k_D values of CO_2 for the plasticized membranes were taken as volume averaged values of the two components. Similar calculations were used to determine the corresponding values of k_D for O_2 (2.18×10^{-3}cm^3 (STP)/cm^3 cmHg) (Tables 6 and 7) and N_2 (1.46×10^{-3} cm^3 (STP)/cm^3 cmHg) by using the data of χ and $\overline{V}_1$ reported by Budzien et al.[32] and Yen and McKetta.[42]

It is important to point out that the calculated value for k_D shown in Table 4 for the solubility coefficient of CO_2 in TCP is 0.0168 cm^3 (STP)/cm^3 cm Hg, is in excellent agreement with those determined experimentally by sorption and NMR measurements indicated above.

From the changes of the gas concentration with pressure in the upstream chamber we can determine its derivative at the limit of zero pressure which, according to the corresponding derivative $(dC/dp)_{p=0}$ from eq 10, is equivalent to $S_0 = k_D + C'_H b$. The experimental values are graphically represented as a function of the weight fraction of TCP in Figure 10, and the corresponding values of $C'_H b$ are shown in the last column of Tables 4−7 for the solubility of CO_2 and O_2 in the different membranes.

From these tables, it is worth noting the important contribution to the total solubility of the gas in the Langmuir sites, much more significant in the case of the 6FDA-TMPD membranes, where the $C'_H b/k_D$ ratio for CO_2 in the pure membrane is about 717 whereas in the pure Matrimid it is only 40, decreasing in an approximately exponential manner with the weight fraction of TCP, as indicated in Figure 11.

Table 6. Values of Solubility Parameters, Interaction Parameters, Henry Solubility Coefficients, and Langmuir Coefficients for the Oxygen Sorption in Matrimid Membranes Plasticized with Tricresylphosphate, at 30 °C

Matrimid	TCP $(1 - w_p)$ feed	TCP $(1 - w_p)$ by TGA	χ	δ_2, $MPa^{1/2}$	$10^3 k_D$, cm^3 (STP)/cm^3 cmHg	$C'_H b$, cm^3 (STP)/cm^3 cmHg
1	0	0	3.04	22.1	0.465	0.0101
2	0.05	0.04			0.55	0.0086
3	0.16	0.155			0.746	0.0048
4	0.20	0.197			0.82	0.0028
5	0.33	0.358			0.964	
6	0.50	0.336			1.07	0.00116
7	1	1	1.65	18.8	2.18	0

Table 7. Values of Solubility Parameters, Interaction Parameters, Henry Solubility Coefficients and Langmuir Coefficients for the Oxygen Sorption in 6FDA-TMPD Membranes Plasticized with Tricresylphosphate, at 30 °C

6FDA-TMPD	TCP$(1 - w_p)$ feed	TCP$(1 - w_p)$ by TGA	χ	δ_2, $MPa^{1/2}$	$10^3 k_D$, cm^3 (STP)/cm^3 cmHg	$C'_H b$, cm^3 (STP)/cm^3 cmHg
1	0	0	5.57	26.5	0.036	0.037
2	0.05	0.05			0.15	0.020
3	0.16	0.157			0.40	0.0090
4	0.20	0.177			0.45	0.0075
5	0.33	0.264			0.65	0.0036
6	1	1	1.65	18.8	2.18	0

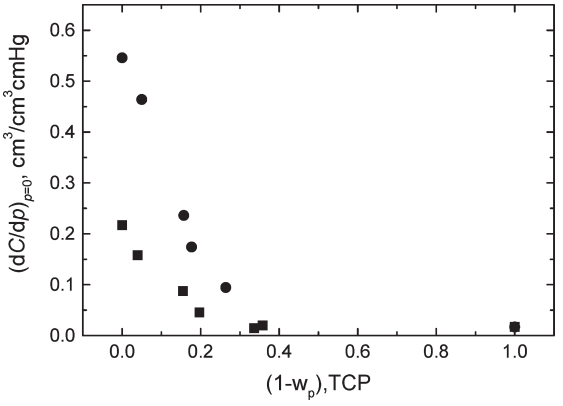

Figure 10. Variation of the derivative of the gas concentration with respect to the pressure in the limit of zero pressure as a function of the weight fraction of tricresylphosphate in the membranes. Matrimid: filled squares. 6FDA-TMPD: filled circles.

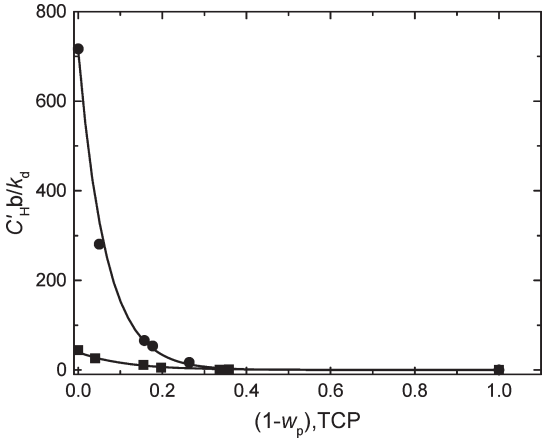

Figure 11. Variation of the ratio $C'_H b/k_D$ with the weight fraction of tricresylphosphate for CO_2 permeation experiments. Matrimid (squares) and 6FDA-TMPD (circles) are shown; the lines are first order exponentials used to join the experimental points but in principle without physical meaning.

Values of the permeability, diffusion, solubility coefficients and permselectivities at the limit of zero pressure for the different membranes and gases are shown in Tables 8 and 9 and Figures 12 and 13, as a function of the weight fraction of TCP.

The comparative analysis of the transport coefficients obtained with this pressure method for CO_2 in the pure polyimide membranes with those determined by sorption and PFG-NMR experiments indicated above in Table 3, shows that a good agreement has been obtained for all the transport coefficients in the case of the 6FDA-TMPD membrane, what seems to indicate the validity of all the procedures and the reliability of the obtained results. For the commercial polyimide membrane, given the low gas solubility and diffusion coefficient, there are greater differences between the results determined by the different procedures, although the value of the most important coefficient, the permeability, is practically identical independently of the used method: pressure or PFG-NMR.

The diffusion coefficient for CO_2 in pure TCP was considered to be equivalent to that obtained for $[^{13}C]O_2$ by PFG-NMR measurements whereas the corresponding values for O_2 and N_2 were determined by considering that the fractional Stokes−Einstein equation[43] for Brownian particles in a liquid is accomplished with:

$$D = \frac{k_b T}{n\pi\eta r} \qquad (14)$$

Table 8. Values of Permeability, Diffusion, and Solubility Coefficients of Carbon Dioxide and CO_2/O_2, CO_2/N_2, and O_2/N_2 Permselectivities in Matrimid Membranes Plasticized with Tricresylphosphate, at 30 °C

Matrimid membranes	TCP $(1 - w_p)$	P, barrers	$10^7 D$, cm^2/s	$S = C'_H b + k_D$, cm^3 (STP)/cm^3 cmHg	P_{CO_2}/P_{O_2}	P_{CO_2}/P_{N_2}	P_{O_2}/P_{N_2}
1	0	7.6	0.032	0.237	4.58	26.57	5.80
2	0.04	5.67	0.036	0.158	4.68	29.38	6.28
3	0.155	1.98	0.023	0.088	4.21	24.44	5.79
4	0.197	1.16	0.026	0.045	3.62	19.02	5.25
5	0.358			0.021			
6	0.336	0.59	0.041	0.0144	3.98	16.86	4.27
7	1	603	35.9	0.0168	8.34	12.67	1.52

Table 9. Values of the Permeability, Diffusion, and Solubility Coefficients of Carbon Dioxide and CO_2/O_2, CO_2/N_2, and O_2/N_2 Permselectivities in 6FDA-TMPD Membranes Plasticized with Tricresylphosphate, at 30 °C

6FDA-TMPD membranes	TCP $(1 - w_p)$	P, barrers	$10^7 D$, cm^2/s	$S = C'_H b + k_D$, cm^3 (STP)/cm^3 cmHg	P_{CO_2}/P_{O_2}	P_{CO_2}/P_{N_2}	P_{O_2}/P_{N_2}
1	0	783	1.435	0.546	4.60	15.8	3.43
2	0.05	248.5	0.536	0.463	4.95	12.6	2.57
3	0.157	52.2	0.222	0.235	5.61	16.3	2.91
4	0.177	42.2	0.242	0.174	3.52	12.1	3.46
5	0.264	19	0.201	0.094	5.94	12.7	2.15
6	1	603	35.9	0.0168	8.34	12.67	1.52

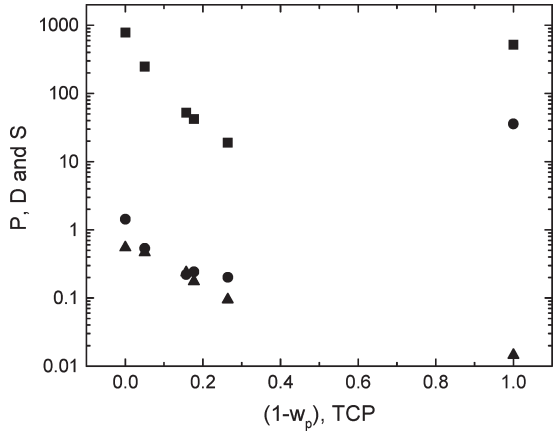

Figure 12. Changes in the permeability in barrers (squares), diffusion in 10^7 cm^2 s^{-1} (circles) and solubility coefficients in cm^3 (STP)/(cm^3 cmHg) (triangles) with the weight fraction of tricresylphosphate in 6FDA-TMPD membranes for carbon dioxide permeation experiments.

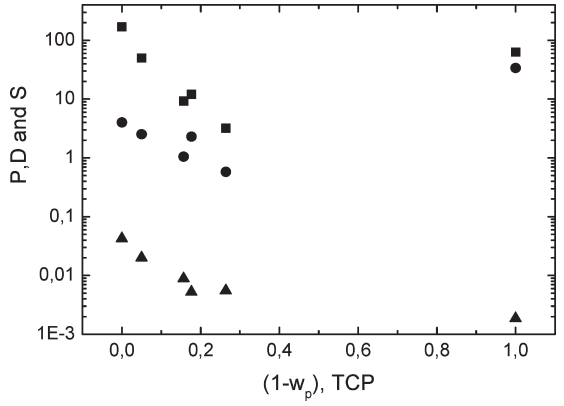

Figure 13. Changes in the permeability in barrers (squares), diffusion in 10^7 cm^2 s^{-1} (circles) and solubility coefficients in cm^3 (STP)/(cm^3 cmHg) (triangles) with the weight fraction of tricresylphosphate in 6FDA-TMPD membranes for oxygen permeation experiments.

where k_b is the Boltzmann constant, η the viscosity of the medium, r is the radius of the particle considered spherical, n is a viscosity dependent parameter $n = n_0\eta^{(\alpha-1)}$, with n_0 being the value of n at unit viscosity and α being a coefficient that indicates the deviation of the pure Stokes−Einstein law ($\alpha = 1$), variable for each solute and very dependent on its size. Taking into account that the molecular size of the three gases studied is similar, then by considering the hydrodynamic radius of CO_2 as 1.65 Å[44] with a value of $D = 3.59 \times 10^{-6}$ cm^2 s^{-1} experimentally determined, and by using the kinetic diameters of O_2 and N_2,[45] values of 3.38×10^{-6} cm^2 s^{-1} and 3.28×10^{-6} cm^2 s^{-1}, respectively, were calculated for their diffusion coefficients and 72 and 47 barrers for their corresponding permeability coefficients in TCP.

As can be seen in Tables 8 and 9, the permeability coefficients of Matrimid present similar values to those reported by others[46] whereas for the 6FDA-TMPD they are within the same order of magnitude,[47] being much higher for the 6FDA-TMPD in comparison with Matrimid, with values exceeding 2 orders of magnitude. The reasons for this behavior are the higher fraction of nonequilibrium excess free volume in the glassy state for the 6FDA-TMPD membranes that permits higher gas adsorption in the Langmuir sites, and also higher diffusion coefficients. The results obtained for the transport coefficients in the plasticized membranes, shown in Tables 8−11, point out the large influence of the plasticizer, with a decrease in all coefficients, including diffusion, with the corresponding decrease in the gas flow and with virtually no influence on the permselectivity.

dx.doi.org/10.1021/ma2005876 |*Macromolecules* 2011, 44, 3862–3873

Table 10. Solubility and Diffusion Contributions to CO_2/O_2, CO_2/N_2, and O_2/N_2 Permselectivities in Matrimid Membranes Plasticized with Tricresylphosphate, at 30 °C

Matrimid membranes	TCP $(1 - w_p)$	$10^7 Dco_2$, cm^2/s	$Sco_2 = C'_H b + k_D$, cm^3 (STP)/cm^3 cmHg	S_{CO_2}/S_{O_2}	S_{CO_2}/S_{N_2}	S_{O_2}/S_{N_2}	D_{CO_2}/D_{O_2}	D_{CO_2}/D_{N_2}
1	0	0.032	0.217	21.42	33.54	1.56	0.21	0.79
2	0.04	0.037	0.158	18.37	27.15	1.48	0.25	1.08
3	0.155	0.024	0.088	17.76	32.37	1.82	0.24	0.76
4	0.197	0.028	0.045	15.61	19.83	1.27	0.23	0.96
6	0.336	0.034	0.0144	10.83	21.49	1.98	0.37	0.78
7	1	35.9	0.0168	7.83	11.51	1.47	1.06	1.10

Table 11. Solubility and Diffusion Contributions to CO_2/O_2, CO_2/N_2, and O_2/N_2 Permselectivities in 6FDA-TMPD Membranes Plasticized with Tricresylphosphate, at 30 °C

6FDA membranes	TCP $(1 - w_p)$	$10^7 Dco_2$, cm^2/s	$Sco_2 = C'_H b + k_D$, cm^3 (STP)/cm^3 cmHg	S_{CO_2}/S_{O_2}	S_{CO_2}/S_{N_2}	S_{O_2}/S_{N_2}	D_{CO_2}/D_{O_2}	D_{CO_2}/D_{N2}
1	0	1.435	0.546	12.84	17.75	1.38	0.36	0.89
2	0.05	0.536	0.463	23.17	34.11	1.47	0.21	0.37
3	0.157	0.222	0.235	26.53	34.51	1.30	0.21	0.47
4	0.177	0.242	0.174	33.39	28.69	0.86	0.10	0.42
6	0.264	0.201	0.094	17.11	36.74	2.15	0.35	0.35
7	1	2.36	0.0168	7.83	11.51	1.47	1.06	1.10

CONCLUSIONS

The most important conclusions that can be extracted from this work are the following:

Precise measurements of the specific volumes of the membranes in the glassy state have permitted the determination of the fraction of nonequilibrium excess free volume in the glassy state, intimately correlated with the gas adsorption in the Langmuir sites.

The Henry solubility coefficients of the pure and plasticized polymer membranes were determined in the glassy state by using gas, plasticizer and polymer solubility parameters, and the Flory−Huggins theory, commonly employed for solutions. At the same time, the CO_2 solubility coefficient calculated in the liquid TCP was in very good agreement with that experimentally obtained by sorption and NMR methods.

The contribution of the Henry solubility coefficients to the total gas solubility is not very important for both Matrimid and 6FDA-TMPD membranes, being in the latter case practically negligible in comparison to the adsorption in Langmuir sites.

Sorption, NMR and permeation measurements of carbon dioxide transport coefficients determined with the three procedures were in fair agreement for the liquid TCP and the pure Matrimid and 6FDA-TMPD membranes.

All the results clearly indicate that the presence of the plasticizer produces a decrease of the oxygen, nitrogen and carbon dioxide permeability coefficients with little influence on the perm-selectivity and, consequently, it does not favor the development of new membranes with high separation performance. Moreover, the presence of the diluent may be clearly detrimental to other membrane properties, such as thermal stability and mechanical resistance.

ACKNOWLEDGMENT

The financial support provided by the CYCIT through Projects MAT2008-06725-C03-01 and MAT2010-20668 is gratefully acknowledged.

REFERENCES

(1) Paul, D. R.; Yampolskii, Y. P.; Eds. *Polymeric Gas Separation Membranes*: CRC Press: Boca Raton FL, 1994.

(2) Freeman, B. D., Pinau, I., Eds. *Polymer Membranes for Gas and Vapor Separation*; ACS Symposium Series 733; American Chemical Society: Washington DC, 1999.

(3) Yampolskii, Y.; Pinau, I.; Freeman, B. D.; Eds. *Materials Science of Membranes for Gas and Vapor Separation*; Wiley: Chichester, West Sussex, U.K., 2006.

(4) Chung, T. S.; Kafchinsky, E. R. *J. Appl. Polym. Sci.* **1997**, *65*, 1555–1569.

(5) Coleman, M. R.; Koros, W. J. *Macromolecules* **1999**, *32*, 3106–3113.

(6) Wang, R.; Cao, C.; Ghung, T. S. *J. Membr. Sci.* **2002**, *198*, 259–271.

(7) Bas, C.; Mercier, R.; Sánchez-Marcano, J.; Neyertz, S.; Alberola, N. D.; Pinel, E. *J. Polym. Sci. B: Polym. Phys.* **2005**, *43*, 2413–2426.

(8) Recio, R.; Palacio, L.; Prádanos, P.; Hernández, A.; Lozano, A. E.; Marcos, A.; de la Campa, J. G.; de Abajo, J. *J. Membr. Sci.* **2007**, *293*, 22–28.

(9) Maeda, Y.; Paul, D. R. *J. Polym. Sci., Part B: Polym. Phys.* **1987**, *25*, 1005–1016.

(10) Larocca, N. M.; Pessan, L. A. *J. Membr. Sci.* **2003**, *218*, 69–92.

(11) García, A.; Iriarte, M.; Uriarte, C.; Iruin, J. J.; Etxebarría, A.; del Río, C. *Polymer* **2004**, *45*, 2949–2957.

(12) Kita, H.; Inada, T.; Tanaka, K.; Okamoto, K. *J. Membr. Sci.* **1994**, *87*, 139–147.

(13) Bos, A.; M. Punt, I. G.; Wessling, M.; Strathmann, H. *Separation Purif. Technol.* **1998**, *14*, 27–39.

(14) Liu, Y.; Pan, C. Y.; Ding, M. X.; Xu, J. P. *J. Appl. Polym. Sci.* **1999**, *73*, 521–526.

(15) Rezac, M. E.; Schoberl, B. *J. Membr. Sci.* **1999**, *156*, 211–222.

(16) Liu, Y.; Wang, R.; Chung, T. S. *J. Membr. Sci.* **2001**, *189*, 231–239.

(17) Staudt-Bickel, C.; Koros, W. J. *J. Membr. Sci.* **1999**, *155*, 145–154.

(18) Chung, T.-S.; Ren, J.; Wang, R.; Li, D.; Liu, Y.; Pramoda, K. P.; Cao, C.; Loh, W. W. *J. Membr, Sci.* **2003**, *214*, 57–69.

(19) Muñoz, D.; de Abajo, J.; de la Campa, J. G.; Lozano, A. E. *Macromolecules* **2007**, *40*, 8225–8232.

(20) Tiemblo, P.; Guzmán, J.; Riande, E.; Salvador, E. F.; Peinado, C. *J. Polym. Sci. B: Polym. Phys.* **2001**, *39*, 786–795. Tiemblo, P.; Guzmán, J.; Riande, E.; Mijangos, C.; Reinecke, H. *Macromolecules* **2002**, *35*, 420–424.
(21) Koros, W. J.; Paul, D. R.; Rocha, A. A. *J. Polym. Sci.: Polym. Phys. Ed.* **1976**, *14*, 687–702.
(22) Stejskal, E. O.; Tanner, J. E. *J. Chem. Phys.* **1965**, *42*, 288–292.
(23) Callaghan, P. T.; Jolley, K. W.; Trotter, C. M. *J. Magn. Reson.* **1980**, *39*, 525–527.
(24) Blochowicz, Th.; Karle, C.; Kudlik, A.; Medick, P.; Roggatz, I.; Vogel, M.; Tschirwitz, Ch.; Wolber, J.; Senker, J.; Rössler, E. *J. Phys. Chem. B* **1999**, *103*, 4032–4044.
(25) Ruiz-Treviño, F. A.; Paul, D. R. *J. Polym. Sci., Part B: Polym. Phys.* **1998**, *36*, 1037–1050.
(26) Maeda, Y.; Paul, D. R. *J. Polym. Sci., Part B: Polym. Phys.* **1987**, *25*, 957–980.
(27) Garrido, L.; López-González, M.; Riande, E. *J. Polym. Sci., Part B: Polym. Phys.* **2010**, *48*, 231–235.
(28) Garrido, L.; López-González, M.; Saiz, E.; Riande, E. *J. Phys. Chem.* **2008**, *112*, 4253–4256.
(29) Crank, J., In *The Mathematics of Diffusion*; Oxford University Press: Oxford, U.K., 1975; p 51.
(30) Vieth, W. R.; Sladek, K. J. *J. Colloid. Sci.* **1965**, *20*, 1014–1033.
(31) Tlenkopatchev, M.; Vargas, J.; Almaraz-Girón, M. A.; López-González, M.; Riande, E. *Macromolecules* **2005**, *38*, 2696–2703.
(32) Budzien, J. L.; McCoy, J. D.; Weinkauf, D. H.; LaViolette, R. A.; Peterson, E. S. *Macromolecules* **1998**, *31*, 3368–3371.
(33) Lin, H.; Freeman, B. D. *J. Membr. Sci.* **2004**, *239*, 105–117.
(34) DiPaola-Baranyi, G.; Guillet, J. E. *Macromolecules* **1978**, *11*, 228–235.
(35) Fleming, G. K.; Koros, W. J. *Macromolecules* **1986**, *19*, 2285–2291.
(36) Merkel, T. C.; Bondar, V. I.; Nagai, K.; Freeman, B. D.; Pinnau, I. *J. Polym. Sci., Part B: Polym. Phys.* **2000**, *38*, 415–434.
(37) Camper, D.; Scovazzo, P.; Koval, C.; Noble, R. *Ind. Eng. Chem. Res.* **2004**, *43* (12), 3049–3054.
(38) Jiang, L. Y.; Chung, T. S.; Rajagopalan, R. *Chem. Eng. Sci.* **2008**, *63*, 204–216.
(39) Kanehashi, S.; Nakagawa, T.; Nagai, K.; Duthie, X.; Kentishand, S.; Stevens, G. *J. Membr, Sci.* **2007**, *298*, 147–155.
(40) Booser, R., Ed. *Handbook of Lubrication. Theory and Design, Vol II: Theory and Design*; CRC: New Hampshire, 1988; p 242.
(41) Reid, R. C.; Prausnitz, J. M.; Poling, B. E., *The Properties of Gases and Liquids*: McGraw-Hill: New York, 1987.
(42) Yen, L. C.; McKetta, J. J., Jr. *AIChE J.* **1962**, *8*, 501–507.
(43) Kenneth, R. H., *J. Chem. Phys.* **2009**, *131*, 054503 and references therein.
(44) Ritter, N.; Antonietti, M.; Thomas, A.; Senkovska, I.; Kaskel, S.; Weber, J. *Macromolecules* **2009**, *42* (21), 8017–8020.
(45) Pillai, R. S.; Peter, S. A.; Jasra, R. V. *Microporous Mesoporous Mater.* **2008**, *113*, 268–276.
(46) Bos, A.; Pünt, I. G. M.; Wessling, M.; Strathmann, H. *Sep. Purif. Technol.* **1998**, *14*, 27–39.
(47) Liu, W.-H.; Chung, T.-S. *J. Membr. Sci.* **2001**, *186*, 183–193.